Role of Myristylation in HIV-1 Gag Assembly†

Fadila Bouamr,‡,§ Suzanne Scarlata,‖ and Carol Carter*,‡

Departments of Molecular Genetics & Microbiology and Physiology & Biophysics, Stony Brook University, Stony Brook, New York 11794

Received December 10, 2002; Revised Manuscript Received March 13, 2003

ABSTRACT: Assembly of the human immunodeficiency virus type 1 (HIV-1) first occurs on the plasma membrane of host cells where binding is driven by strong electrostatic interactions between the N-terminal matrix (MA) domain of the structural precursor polyprotein, Gag, and the membrane. MA is also myristylated, but the exact role this modification plays is not clear. In this study, we compared the protein oligomerization and membrane binding properties of Myr^+ and Myr^- Gag^{MA} expressed in COS-1 cells. Sedimentation studies in solution showed that both the myristylated Gag precursor and the mature MA product were detected in larger complexes than their unmyristylated counterparts, and the myristylated MA protein bound liposomes with ~3-fold greater affinity than unmyristylated MA. Aromatic residues near the N-terminal region of the MA protein were more accessible to chymotrypsin in the unmyristylated form and, consistent with this, an epitope in the N-terminal region was more exposed. Moreover, the cyclophilin binding site in the CA domain downstream of MA was more accessible in the unmyristylated Gag protein, while the Tsg101 binding site in the C-terminal region was equally available in the unmyristylated and myristylated Gag proteins. Taken together, our results suggest that myristylation promotes assembly by inducing conformational changes and facilitating MA multimerization. This observation offers a novel role for myristylation.

The HIV-1 structural precursor polyprotein ($Pr55^{Gag}$) is thought to bind the plasma membrane of host cells through a cluster of positively charged residues in its N-terminal matrix (MA) domain and through modification by co-translational N-terminal myristylation (*1*, *2*). Recently, myristylation was shown to be a critical determinant to target Gag to cholesterol- and sphinglomyelin-enriched microdomains (rafts) on the plasma membrane (*3*). Removal of the myristate signal results in improper targeting of Gag to the soluble pool or to intracellular membranes (*1*, *4*−*6*). Gag plasma membrane binding is followed by assembly and release of the viral particle. During the virus maturation stage that follows, proteolytic processing of assembled Gag by the viral-encoded protease (PR) results in formation of mature Gag cleavage products including myristylated MA (Myr^+ MA). Most of the MA protein forms a shell that underlies the lipid bilayer obtained when the assembled virus buds through the plasma membrane during release from the cell (*7*, *8*). A subpopulation of MA is hypothesized to dissociate from the membrane and direct transport of a viral preintegration complex to the nucleus (*9*, *10*), but this notion is controversial (*11*). To reconcile the apparently opposing membrane- and nuclear-targeting functions of MA, it has been suggested that conformational changes in MA following proteolytic maturation result in sequestration of the myristate group (*2*). Currently, this myristyl switch hypothesis is based on observations that MA in the context of the Gag precursor binds more strongly to membrane than mature MA (p17), as assayed by subcellular localization or binding to membrane-enriched cell fractions or liposomes (*12*−*15*). In general, these observations are interpreted to reflect a reduction in exposure of the myristate moiety, which in turn prevented the presumed stabilizing effects of fatty acid insertion into the lipid bilayer. This gives the impression that strong binding is mediated through the modification itself. However, while myristate contributed all of the membrane binding energy in an assay using acylated peptides, it is intrinsically a weak binding signal (*16*). Other determinants contribute in the case of some retroviral Gag proteins. Genetic analyses show that basic residues contribute to membrane binding of both the HIV-1 Gag precursor and the mature protein (*2*). Gag and MA lacking myristate still show strong salt-dependent affinity for negatively charged liposomes (*17*). The binding energy in proteins containing both a myristate and a basic cluster reflects a combined contribution from both determinants and is much greater than the signal from either motif alone. In the case of other retroviral Gag polyproteins such as the Rous sarcoma virus (RSV) and human T-cell leukemia virus type 1 (HTLV-I) Gag proteins that are myristylated but do not contain an obvious cluster of N-terminal basic residues, proper folding of the protein brings together scattered basic residues on an exposed hydrophobic face of the molecule (*2*, *18*, *19*). This could be achieved in vivo only when the proteins are myristylated in the natural milieu. Taken together, these observations suggest that structural differences resulting from the presence of myristate, rather

† This work was supported by NIH Grant GM58271 to S.S. and C.C.

* Address correspondence to the following author. Telephone: (631) 632-8801. Fax: (631) 632-9797. E-mail: ccarter@ms.cc.sunysb.edu.

‡ Department of Molecular Genetics & Microbiology.

§ Present address: Howard Hughes Medical Institute, Columbia University/Biochemistry, 701 W. 168th St. (HHSC 1313), New York, NY 10023.

‖ Department of Physiology & Biophysics.

10.1021/bi020692z CCC: $25.00
Published on Web 05/09/2003

than the element alone, are responsible for the binding properties.

The 3-dimensional structure of unmyristylated (Myr^-) HIV-1 MA has been determined by both NMR and X-ray crystallography and shown to be predominantly composed of a globular core of clustered helices joined by loops or regions of extended structure (*20*−*22*). This general structure appears to be conserved among retroviruses (*23*−*26*). The front face of the protein is highly basic allowing strong interaction with electronegative lipid headgroups. X-ray crystallography showed the MA protein to be a trimer, an organization that is supported by solution analysis of recombinant unmyristylated proteins purified from bacteria (*27*) or insect cells (*28*). Interestingly, the MA protein of the closely related equine infectious anemia virus (EIAV) lacks myristylation but is otherwise highly structurally and functionally homologous (*29*, *30*). EIAV MA protein appears to have a both a basic membrane-binding face that exhibits strong salt dependency and a second hydrophobic membrane-binding site (*29*, *30*). The expectation of different structures for the myristylated and unmyristylated HIV-1 Gag and MA proteins is not unwarranted. N-terminal myristylation occurs co-translationally on soluble ribosomes (*31*, *32*). The aliphatic modification will therefore have been attached to its N-terminal Gly acceptor before completion of protein synthesis, which may promote sequestration of the hydrophobic chain away from the cytosol and into the protein structure. Consistent with this idea, the HTLV-I Gag protein was found to be cytosolic, suggesting that the myristyl moiety is unavailable for binding membranous vesicles in the cytoplasm (*33*). The structure of myristylated proteins whose structure has been solved by NMR or X-ray crystallography [e.g., recoverin (*34*−*36*); HIV-1 Nef (*37*); and poliovirus VP4 (*38*, *39*)] show sequestration of the fatty acid moiety within a hydrophobic pocket. This sequestering event apparently impacts the structure of downstream sequences as differences in the structure of the modified and unmodified forms extend well beyond the pocket. In recoverin, the myristic acid is sequestered in a deep hydrophobic box where it is clamped by interaction with multiple residues. The comparison of the myristylated and the unmyristylated forms of the protein showed that the N-terminal region that is composed of two helices in the Myr^+ protein is longer and more flexible than the same region in the Myr^- protein, where it is more defined and rigid. In this case, sequestering of the myristate stabilized a conformation of the molecule that provided greater fluidity. It is suggested that this enhanced flexibility facilitates switching between myristate-exposed and -sequestered states, and thereby, the proper functioning of the molecule. The myristylated form of the Nef protein adopts a compactly folded structure in which the myristic acid moiety is tucked toward the inside of the protein by formation of a loop between residues Gly2 and Trp5. In contrast, the unmyristylated Nef protein displays an extended N-terminal area where the first two helices are destabilized. The myristylated structure appears to be important for multimerization of the protein, as it has been shown that Nef interaction with actin to form a high molecular mass complex is dependent on the N-terminal modification (*40*). Myristylation of poliovirus VP4 results in the formation of a twisted tube structure stabilized by interaction between the Gly2 residue carrying the myristic acid and the Thr28 in the core of the protein. This sequestering of the myristic acid is required for the pentameric assembly of VP4. Mutation of Thr28 disturbs the twisted tube structure, resulting in abnormal assembly of the virus. This implies that the torsion imposed by the sequestering of the myristic acid affects the subunit interactions essential to proper assembly of the poliovirus particle. Together, these observations indicate that the myristyl moiety and its sequestration in the hydrophobic core of the molecules confer defined conformations to the proteins that influence protein−protein interactions and function.

In contrast to the well-characterized examples above of myristylated proteins that sequester the fatty acid moiety, the structure of myristylated MA protein has not yet been determined. In this report, we compared biochemical and biophysical properties of myristylated and unmyristylated HIV-1 Gag and MA proteins in the cytosol of transfected COS-1 cells. Our results indicate differences in the N-terminal region of mature MA, and in the context of the Gag precursor, differences that extended beyond the MA domain. The modification influenced the membrane binding of MA to a slightly greater extent than Gag, suggesting that the precursor may contain binding determinants outside of MA. This may provide an explanation for the observation, noted above, that MA in the context of the Gag precursor binds membrane better than mature MA. These findings support the idea that the modification may influence the presentation of specific regions in the structure or affect multimerization properties and thereby determine the overall functional characteristics of the protein.

MATERIALS AND METHODS

Cell Culture, Transfection, and Preparation of Cytoplasmic Extracts. COS-1 cells were cultured in DMEM[1] supplemented with fetal bovine serum to 60% confluency at 37 °C. The cells were transfected with *p*CMV-*rev* and *p*pgRRE-r encoding wild-type *gag* (*41*) or with a plasmid encoding *gag*G2A (Myr^- Gag, refs *42* and *43*) using the FuGENE 6 reagent (Roche) according to the instructions of the manufacturer. pCMV-*rev* encodes Rev, a regulatory viral protein required for cytoplasmic expression of Gag and Gag-Pol mRNAs (*41*). At 48 h post-transfection, the cells were harvested by scraping into cold PBS and pelleted. The pelleted cells were washed three times with cold PBS, allowed to swell in 1 mL of cold hypotonic buffer (10 mM Tris, pH 7.4, 1 mM $MgCl_2$) containing protease inhibitors for 15 min on ice, and disrupted with 35 strokes of a Dounce homogenizer with a type B pestle. The total lysate was spun for 10 min at 1000*g* at 4 °C to remove unbroken cells and nuclei. Where indicated in the text, the supernatant (S1 extract) was centrifuged at 100 000*g* for 30 min to obtain the soluble (S100) fraction and a plasma membrane-enriched (P100) fraction (*44*).

Sedimentation Analysis. Cytoplasmic (S100) extract was applied to 10−50% sucrose gradients prepared in hypotonic buffer (10 mM Tris, pH 7.4, 1 mM $MgCl_2$), and the samples were centrifuged for 20 h at 48 000 rpm in a SW 50.1 rotor and Beckman ultracentrifuge. After centrifugation, fractions were collected from the top of the tube, the refractive index

[1] Abbreviations: DMEM, Dulbecco minimal essential medium; PBS, phosphate-buffered saline; SDS−PAGE, sodium dodecyl sulfate-polyacrylamide gel electrophoresis; DTT, dithiotreitol.

was measured, and the protein composition was determined by SDS−PAGE and Western analysis. A low molecular weight calibration kit (Amersham) provided sedimentation molecular weight markers.

Immunoprecipitation Assay. Protein A agarose beads (Pierce), pre-washed three times with either cold nondenaturing hypotonic (10 mM Tris, pH 7.4, 1 mM $MgCl_2$) or denaturing RIPA (0.5% Nonidet P-40, 0.5% deoxycholate, 1 mM PMSF, 1 mM Na_2HPO_4, 150 mM NaCl, 10 mM Tris, pH 7.8) buffer containing protease inhibitors (Roche) were incubated with the appropriate antibody, added to cytoplasmic extracts, and rotated at 4 °C for 60 min. Immunoprecipitates were washed in hypotonic or RIPA buffer, boiled in SDS sample buffer with 5% mercaptoethanol, resolved by SDS−PAGE, and analyzed by Western blotting with the antibody indicated in the text.

Limited Proteolytic Digestion. Chymotrypsin digestion of samples was performed using 10 μg of total S100 protein for the period indicated in the text at 37 °C at an enzyme-to-substrate ratio of 1:10. The reaction was stopped by boiling in SDS sample buffer.

Protein Detection. Samples were adjusted to 1% SDS by addition of 5X SDS sample buffer (l mM Tris-HCl, 20% glycerol, 4% SDS, 0.5% Bromo-phenol blue, 500 mM DTT) and heated for 5 min at 95 °C. The proteins in the sample were then resolved by electrophoresis through 12.5% SDS−polyacrylamide gels. Following electrophoresis, the gels were transferred to nitrocellulose and analyzed by Western blotting with the antibodies specified in the text. Monoclonal antibody anti-MA I was a gift of R. Schroenbrunner (Roche, Switzerland). Monoclonal anti-MA Abs was purchased from Advanced BioSciences. Rabbit polyclonal anti-capsid (CA) was raised against a native form of the CA protein (*45*). Sheep monospecific antibody raised against a peptide encompassing aa 95−102 in CA was purchased from International Enzymes. Mouse monoclonal anti-CA antibody was purchased from NEN-DuPont. Anti-cyclophilin A was obtained from BioMol. Anti-Tsg101 monoclonal antibody was obtained from Santa Cruz. Proteins were visualized by chemiluminescence using Lumi-Light reagents (Roche). Where indicated in the text, measurements of relative protein levels were determined by densitometry using NIH Image 1.62 software.

Fluorescence Assays. Sample Preparation. Large unilamellar vesicles (LUVs, 0.1 mm diameter) composed of 1,2-palmitoyl-oleoyl-phosphatidylcholine (PC), -phosphatidylserine (PS), and -phosphatidylethanolamine (PE) at a molar ratio of 1:1:1 were prepared by extrusion (*46*). Myristylated and unmyristylated HIV-1 MA in cytoplasmic extracts were specifically labeled using anti-MA Abs monoclonal antibody tagged with Oregon Green (OG). This antibody recognizes its antigenic site only in the context of the mature MA protein (anti-MA Abs; ref *2*). The anti-MA Abs antibody was labeled by addition of probe from an OG stock in dimethylformate at a probe to protein molar ratio of 4:1. Following overnight incubation at 5 °C, unreacted probe was removed by dialysis against 40 mM Hepes, pH 7.0, 0.5 M NaCl, 1 mM DTT. The labeling ratio was estimated to be 1:1 as determined by absorption spectroscopy and the Bradford colorimetric assay. OG-anti-MA Abs was used at a concentration 2-fold lower than the concentration of MA as measured in independent fluorescence titrations. Myristylated and unmyristylated Gag and MA-CA in cytoplasmic extracts were labeled by the procedure described above using a monospecific antibody raised against the CA protein.

Analysis of Protein−Lipid Binding. Lipid titrations were carried out on the fluorescent-tagged IgG-labeled proteins in cytoplasmic extracts by addition of increasing amounts of PC:PS:PE-LUVs from a concentrated stock. Changes in fluorescence were monitored by recording the spectra at λ_{ex} = 480 nm, scanning from λ_{em} 500−600, and calculating the integrated intensity. Control studies were done using extracts prepared from *rev*-transfected cells. All fluorescence measurements were made using an ISS fluorimeter (I.S.S., Inc., Champaign, IL) with samples contained in microcuvettes with a path length of 3 mm. All samples showed a similar ~15% increase in emission intensity upon membrane binding. This increase was normalized to 1.0 to evaluate the membrane partition coefficient upon addition of lipid.

Homotransfer. Fluorescence homotransfer was measured by monitoring the anisotropy of OG-tagged IgG-labeled protein at λ_{ex} = 480 nm and λ_{em} = 525 nm. Homotransfer is detected by fluorescence anisotropy, which is a measure of the polarization of the emitted light. Data were corrected for background scattering. Measurements were taken by beginning at 0 nM protein and adding small increments up to a total of 200 nM. As the size of the Gag multimers formed during the assembly pathway is unknown, the data was fit by assuming that Gag monomers associate to dimers, trimers, tetramers, or hexamers.

RESULTS

Differential Membrane Binding of Myr$^+$ and Myr$^-$ MA. The Gag and MA proteins that accumulated in the soluble fraction of mammalian cells transfected with wild-type HIV-1 *gag*, *pol*, and *rev* provided a source of myristylated proteins. A subpopulation of the Gag proteins in this fraction are destined for membrane binding and assembly (*47*), while MA proteins that were prematurely cleaved from Gag provide a physiologically relevant model for myristylated MA in lieu of bacterially expressed and unmyristylated protein. Mutated *gag*, encoding Gag, and Gag-Pol proteins in which Ala was substituted for Gly_2 (G_2A) was used to obtain unmodified Gag and MA protein. In the case of the G_2A mutant, comparable amounts of Gag and Gag-related proteins accumulate in the cytoplasm, but the efficiency of membrane-associated assembly is significantly reduced. This is indicated by diminished association of the Gag and MA proteins with plasma membrane-enriched particulate cellular components and the absence of viral particles in the media as we and others have shown previously (*43*, *48*). The extracts prepared from cells transfected with wild-type or mutated *gag* contained full-length $Pr55^{Gag}$ precursor, prematurely proteolytically processed MA-CA cleavage intermediate, and mature CA recognized by anti-CA antibody (Figure 1A, lanes 1 and 3). Neither extract contained viral particles, as indicated by the absence of particulate viral proteins (data not shown). The mature MA-specific anti-MA Abs was used as a probe because it detects only mature Myr$^+$ (lane 2) or Myr$^-$ (lane 4) MA (*2*). This is also evident from its inability to detect the Gag precursor and MA-CA proteins present in the samples.

The membrane binding properties of the Myr$^+$ and Myr$^-$ MA proteins in the soluble fraction were compared by

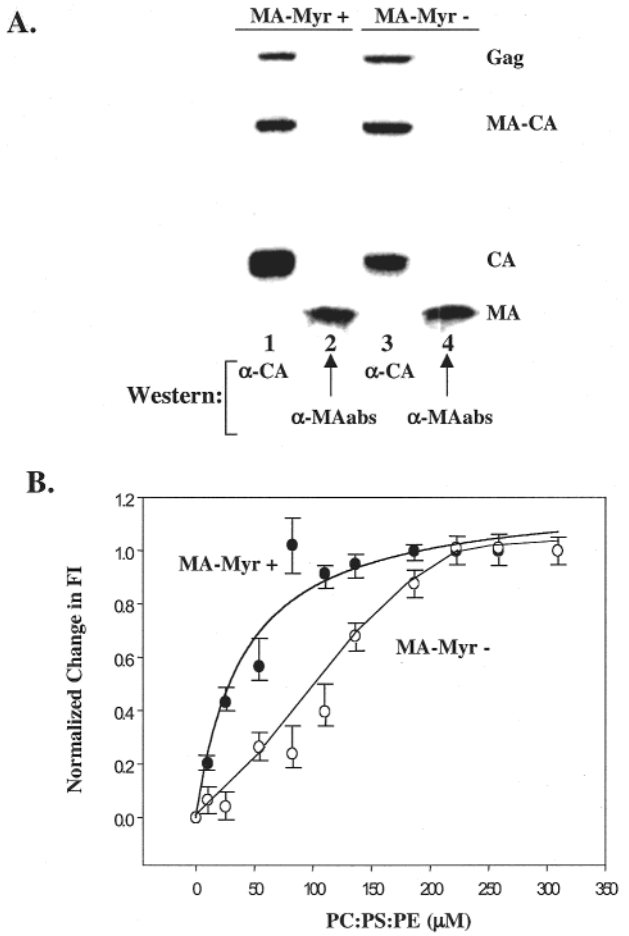

FIGURE 1: (A) Protein composition of cytoplasmic extracts expressing Myr^+ and Myr^- gag. Proteins in S100 extracts were identified by Western analysis with a monospecific antibody against CA (lanes 1 and 3) or MA (lanes 2 and 4) proteins. (B) Membrane binding affinity of Myr^+ and Myr^- MA. Lipid titrations were carried out as described in Materials and Methods, using OG-tagged anti-MA Abs-labeled MA proteins in S100 fractions. Closed circles, Myr^+ MA; open circles, Myr^- MA. Maximal sample error: ±0.08.

measuring the partition coefficient of S100 preparations of the two proteins labeled with fluorescent-tagged Oregon Green (OG) antibody. Previous studies demonstrated that the presence of the IgG antibody and its probe did not alter the binding affinity of recombinant (Myr^-) MA or Gag protein (*27*). Large unimellar vesicles (LUVs) with a significant neutral phospholipid composition were titrated into the OG-anti-MA Abs solution, and the increase in fluorescence intensity as the proteins bind to the membrane was assessed relative to control samples titrated with buffer. No changes in fluorescence intensity were detected with extracts prepared from the control cells transfected with *rev* alone (data not shown). In contrast, as shown in Figure 1B, both samples containing MA proteins bound membranes. The presence of myristate shifted the membrane binding affinity from a midpoint of 110 to 35 μM lipid. Similar results were obtained using a different anti-MA antibody (data not shown), making it unlikely that the difference was due to differential antibody recognition of the Myr^- and Myr^+ proteins. Thus, the Myr^+ MA in the cytosol bound membrane with higher affinity, indicating that the myristate directly or indirectly contributes to binding in the context of the mature protein.

Characterization of the Multimerization State of Myr^+ and Myr^- MA. The Myr^+ MA protein may have assumed a conformation that exposed the regions involved in membrane binding. Alternatively, the putative conformation may have facilitated multimerization and thereby enhanced the presentation of membrane-binding determinants. Differences in protein complex size (or shape) were assessed by their sedimentation behavior in sucrose gradients. The sedimentation of the Myr^+ and Myr^- MA proteins was compared to the sedimentation behavior of marker proteins that provide standards for globular proteins such as MA (*49*−*51*). The mature MA-specific probe, anti-MA Abs (*2*), was used for these studies. As shown in Figure 2A, the Myr^+ and Myr^- MA proteins both sedimented faster than expected for the monomeric protein (17 kDa), based on the sedimentation characteristics of α-lactalbumin (14.4 kDa, lanes 21−26). However, they did not sediment identically. Consistent with previous results obtained with recombinant proteins in insect cells (*28*), the Myr^- MA migrated more slowly than the Myr^+ MA. Myr^- MA (lanes 13−20) sedimented in sucrose between the 43 kDa (lanes 17−21) and 67 kDa (lanes 15−19) markers. Myr^+ MA (lanes 5−12) sedimented ahead of the 94 kDa marker (lanes 14−16), suggesting formation of larger complexes. The results suggest that the Myr^+ and Myr^- MA proteins are components of complexes of different sizes. These distinctions might reflect differences in MA-MA subunit packing as trimers (51 kDa), hexamers (~102 kDa), or larger oligomers or association with cellular proteins or both. Thus, myristylation appears to have favored formation of bigger homo- or heteromeric complexes of MA.

To determine if the differences in sedimentation behavior reflected differences in the multimerization properties of the Myr^+ and Myr^- MA proteins, we used fluorescence homotransfer, which measured fluorescence resonance energy transfer between identical probes attached to the proteins. Mature MA-specific anti-MA Abs was labeled with a fluorophore capable of transferring its energy when one probe is in close proximity to another. The labeled antibody was then titrated into the S100 fraction of COS-1 cells expressing either Myr^+ or Myr^- protein (Figure 2B). The same general behavior was observed for both samples at low probe concentrations (5−25 nM). The addition of more antibody resulted in attachment to subunits on the same multimer causing a decrease in anisotropy because of energy transfer. The Myr^- sample reached a plateau at a lower probe concentration than the Myr^+, which continued to decline until 80 nM. The final amount of homotransfer between the probes attached to the Myr^+ MA complex was greater (i.e., displayed a lower anisotropy) than that of probes attached to the Myr^- MA complex, implying that Myr^+ MA was in a larger complex than Myr^- MA. These observations support the results of the sedimentation assay.

Differential Membrane-Binding and Subunit Packing of Myr^+ and Myr^- Gag/MA-CA. To examine the relationship between myristylation, conformation, and multimerization in the context of the Gag precursor, the contribution of myristate to membrane binding and multimerization in the context of the Gag precursor and MA-CA processing intermediate was assessed. For these experiments, Gag was labeled with OG-tagged anti-CA antibody. Since mature CA does not bind LUVs in the assay (*42*), the probe reflected

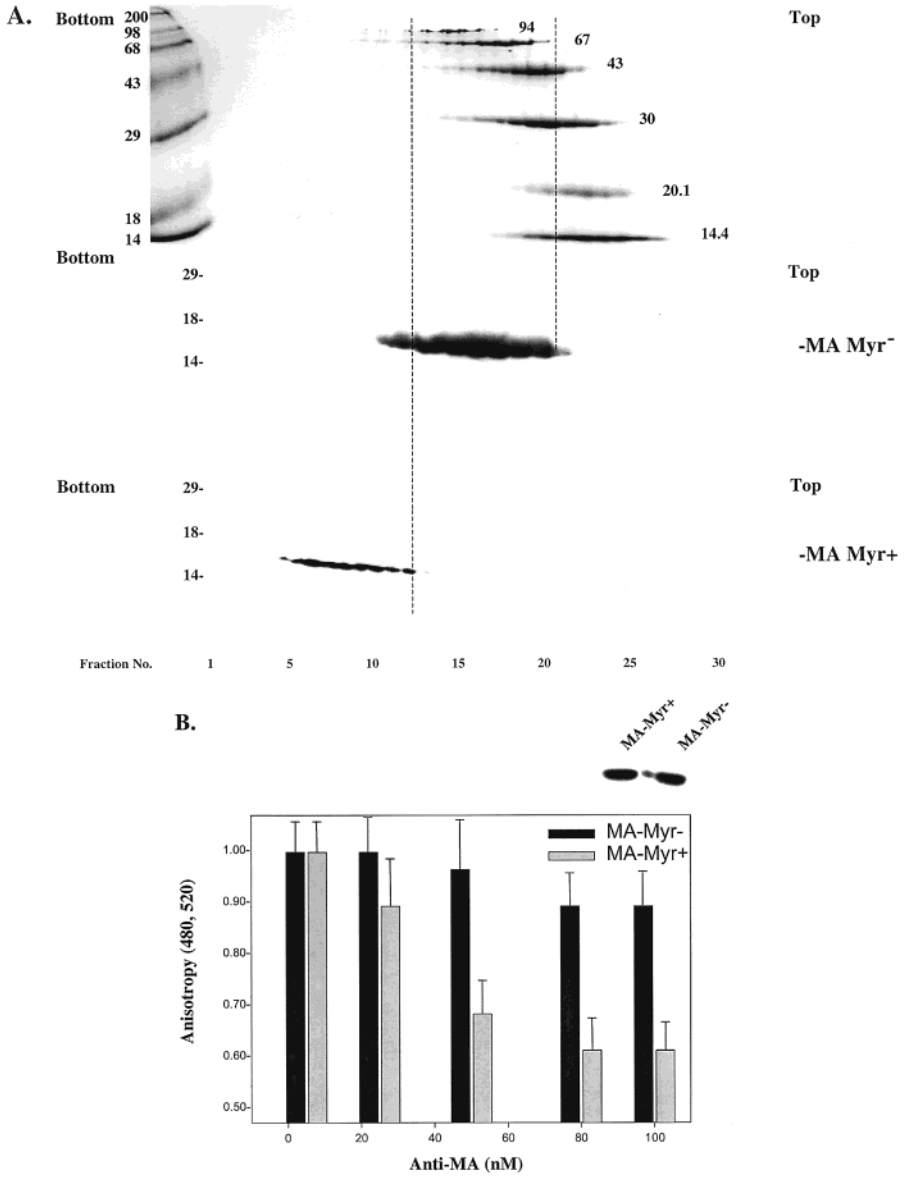

FIGURE 2: Multimerization state of Myr^+ and Myr^- MA protein. (A) Sedimentation in sucrose gradients (the top of the gradient is on the right). S100 extracts containing Myr^+ and Myr^- MA proteins were fractionated on 10−50% sucrose gradients as described in Materials and Methods. Following centrifugation, fractions were collected from the bottom of the gradient, and the protein composition of the fractions was determined by SDS−PAGE and Western analysis with anti-MA Abs. The top panel shows the sedimentation of marker proteins in the sucrose gradient [α-lactalbumin (14.4 kDa), trypsin inhibitor (20.1 kDa), carbonic anhydrase (30 kDa), ovalbumin (45 kDa), albumin (66 kDa), and phosphorylase *b* (97 kDa)]. Molecular weight markers (in kDa) are on the left of the panel. The migration position of the MA protein in the SDS−PAGE is indicated on the right of the panel. The dashed lines show the migration of the MA proteins relative to the markers in the sucrose gradient. Sucrose gradient fraction numbers are indicated on the bottom. (B) Fluorescence homotransfer. Fluorescence homotransfer was measured as described in Materials and Methods using anti-MA Abs antibody tagged with OG. Inset, Western analysis of the extracts showing MA protein detected by the anti-MA Abs antibody. Maximal sample error: ±0.006.

the membrane binding of Gag and MA-CA. To assess membrane binding, LUVs were titrated into the solution as described above, and the increase in fluorescence intensity as the proteins bind to the membrane was determined relative to control samples derived from cells transfected with *rev* alone. As shown in Figure 3A, the difference in membrane affinity between unmyristylated and myristylated Gag proteins is not as large as with the mature MA protein (∼75 and 40 μM, respectively).

The relatively small amount of Gag in the soluble fraction precluded assessment of its sedimentation behavior in sucrose gradients. Therefore, to examine the self-associative properties of the Myr^+ and Myr^- Gag proteins, OG-labeled anti-CA antibody was titrated into the S100 fraction of COS-1 cells expressing either Myr^+ or Myr^- protein, and fluorescence homotransfer was determined (Figure 3B). As was the case with MA, the same general behavior was observed for both the Myr^+ and the Myr^- Gag proteins in that the amount of homotransfer between OG-anti-CA probes was always greater (i.e., displayed a lower anisotropy) when the probes were attached to Myr^+ Gag/MA-CA than Myr^- Gag/MA-CA. The results support the conclusion that Myr^+ Gag/MA-CA is in larger complexes than the unmyristylated counterparts and indicate that the myristate moiety contributes

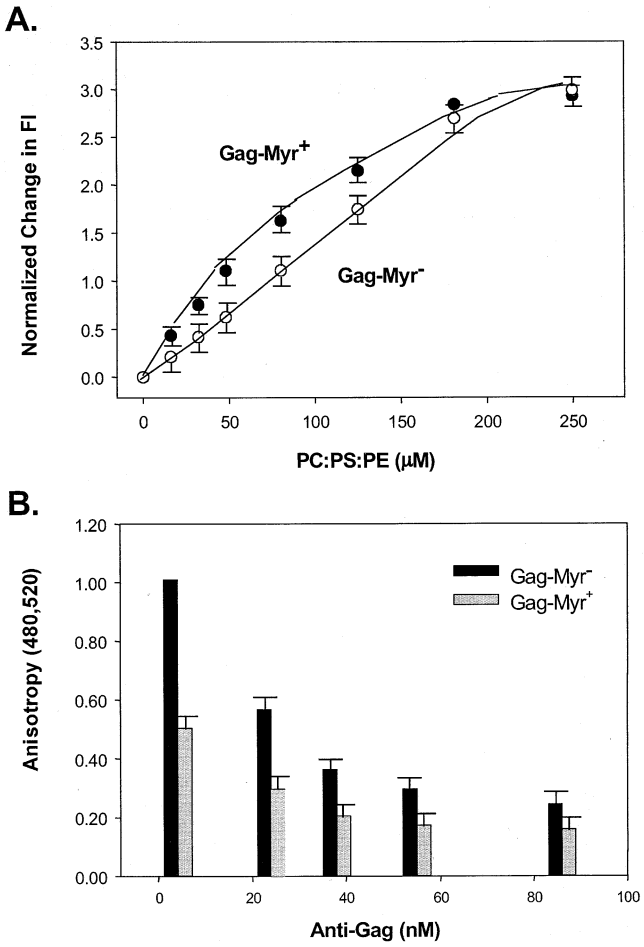

FIGURE 3: Membrane and oligomerization properties of cytosolic Myr^+ and Myr^- Gag/MA-CA proteins. (A) Membrane binding affinity. Lipid titrations were carried out as described in Materials and Methods, using OG-tagged anti-CA-labeled proteins in S100 fractions. Closed circles, Myr^+ Gag; open circles, Myr^- Gag. Maximal sample error: ±0.08. (B) Fluorescence homotransfer. Fluorescence homotransfer was measured as described in Materials and Methods using anti-CA antibody tagged with OG. The antibody detected a protein composition identical to that shown in Figure 1, lanes 1 and 3. Maximal sample error: ±0.006.

tomultimerization in the context of both the Gag precursors and the mature MA protein.

Limited Proteolytic Digestion of Cytosolic Myr^+ and Myr^- MA. The results above suggested that the Myr^+ and Myr^- Gag precursor and the mature MA proteins accumulated in complexes with distinct membrane binding and associative properties. To assess this further, we compared the susceptibility of the proteins to limited chymotryptic digestion. Chymotrypsin was chosen because the aromatic residues that are potential substrates for the enzyme (Trp16, Tyr29, Trp36 and Phe43, Tyr77, and Tyr86, Figure 4, top) are distributed throughout the core of the MA protein and might therefore permit differences in Myr^+ and Myr^- MA to be detected. Limited chymotryptic digestion was performed on the multimeric proteins in the cytosolic fraction. Following incubation with chymotrypsin, the samples were boiled in SDS buffer to denature the proteins, and the undigested proteins and the products of chymotrypsin hydrolysis were separated by SDS−PAGEs. As shown in Figure 4, the Myr^+ and Myr^- MA proteins exhibited similar sensitivity to chymotrypsin during the first 30 min of incubation. The cleaved proteins (~13 kDa, designated by filled circle in

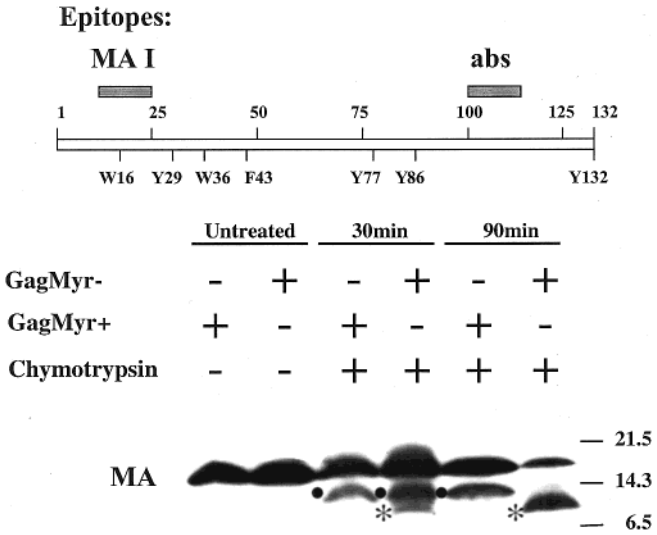

FIGURE 4: Limited proteolytic digestion of Myr^+ and Myr^- MA with chymotrypsin. Top, locations in MA of aromatic residues and the antigenic site recognized by the probe (shaded rectangle). Bottom, chymotrypsin (1 μg) was added to 10 μg of total S100 protein containing Myr^+ or Myr^- MA and incubated for 30 and 90 min at 37 °C. The reaction was stopped by boiling in SDS sample buffer. Proteins were analyzed by SDS−PAGE and Western blotting with MA-specific anti-abs antibody. Molecular weight markers in kDa are indicated on the left of the panel. Filled circle: chymotryptic fragment detected in both samples; *, ~11 kDa chymotryptic fragment detected in the Myr^- MA sample.

the figure) retained the antigenic site of the anti-MA Abs antibody, which is localized to the C-terminal region (data not shown). This indicated that the aromatic residues in the C-terminal portion of both the Myr^+ and the Myr^- MA proteins (Tyr77 and/or Tyr86) were inaccessible to the enzyme. After 90 min, little change was detected in the digest containing the Myr^+ protein. In contrast, the proteins in the sample containing Myr^- MA were further digested to a ~11 kDa fragment (designated by * in the figure). As the 11 kDa fragment retained the C-terminal anti-MA Abs antigenic site, this fragment was generated by cleavage at aromatic amino acids in the N-terminal region of MA (possibly Tyr29 or Trp36), implying that they were more accessible in the Myr^- MA protein as compared to the Myr^+ MA protein. The ~11 kDa fragment was not detected in the Myr^+ MA protein digest, even after long (overnight) exposure. The results suggest that regions in the core of MA were differentially exposed to the chymotrypsin probe in the cytosolic complexes containing the Myr^+ and Myr^- forms of the protein.

MAp17 Epitope Is Exposed Differently in Myristylated Wild-Type and Unmyristylated Mutant MA. Finding apparent differences in the accessibility of core residues in the N-terminal region of Myr^+ and Myr^- MA prompted us to examine the possibility that these proteins were conformationally different in the region near the N-terminal basic region (aa 17−31, ref *2*). To do this, we determined the accessibility of an antigenic site in this region. Monoclonal antibody MA I recognizes an antigenic site that includes residues 11−25, based on studies using recombinant MA-related proteins and synthetic peptides in enzyme linked immunoserological assays (ELISA) and Western analyses (data not shown). Previously, we demonstrated that this antibody recognizes recombinant Myr^- MA purified from

FIGURE 5: Differential accessibility of the anti-MA I antigenic site in Myr$^+$ and Myr$^-$ MA cytosolic complexes. Immunoprecipitation with anti-MA I antibody of S100 extracts under nondenaturating (lanes 1−3) and denaturing (lanes 4−6) conditions. The lanes contain immune-precipitates derived from the S100 extracts of cells transfected with *rev* alone (lanes 1 and 4), or *rev* with wild-type *gag*/*pol* (lanes 2 and 5), or *rev* with Myr$^-$ *gag*/*pol* (lanes 3 and 6). MA proteins were identified by Western blotting with anti-MA abs antibody.

an expression strain of *Escherichia coli* (*27*). Cytoplasmic extracts prepared from transfected mammalian cells expressing the Myr$^+$ and Myr$^-$ MA proteins were subjected to immunoprecipitation with anti-MA I antibody under nondenaturing and denaturating conditions as described in Materials and Methods. As shown in Figure 5, the antibody immune-precipitated only the Myr$^-$ MA protein under nondenaturing conditions (lane 3). In contrast, the antibody precipitated both the Myr$^+$ (lane 5) and the Myr$^-$ (lane 6) MA proteins when the highly denaturing RIPA buffer was used for the immunoprecipitation reaction. The results support the notion that the Myr$^+$ and Myr$^-$ MA proteins are conformationally different in the region of the antigenic site near the membrane-binding signal, or alternatively, that different multimerization states of the Myr$^+$ and Myr$^-$ MA proteins were responsible for the difference in accessibility of the antigenic site.

Distal Effects of N-Terminal Myristylation. Immunoprecipitation with the anti-MA I antibody under nondenaturing conditions followed by Western blotting with anti-CA monoclonal antibody revealed that ∼4-fold more Myr$^-$ Gag protein was precipitated by the antibody than Myr$^+$ Gag (Figure 6A, compare lanes 2 and 3). In contrast, comparable amounts of Myr$^+$ and Myr$^-$ proteins were detected in the supernatant fractions (lanes 5 and 6). The fact that the antigenic site that is recognized by the anti-CA antibody used for Western blotting lies in the CyP A binding region (aa 210−230, ref *42*) raised the possibility that the N-terminal modification had distal effects. To determine if myristate affects the accessibility of cellular protein binding sites in the context of the Pr55^{Gag} precursor, we compared the ability of Myr$^+$ and Myr$^-$ Gag proteins to capture cyclophilin A (CyP A, 17 kDa), which binds residues 217−224 in the CA domain of Gag (*52*) and Tsg101 (46 kDa), which requires the L domain in the C-terminal p6 region of Gag (*53*). Protein A agarose beads coated with anti-CA polyclonal antibody were prepared and incubated with the cytosolic extracts containing the Myr$^+$ or Myr$^-$ Gag-related proteins. Following this incubation period, the samples were analyzed by Western blotting using the same monoclonal anti-CA antibody. Comparable amounts of total CA-related protein derived from Myr$^+$ and Myr$^-$ Gag had been retained on the beads coated with the anti-CA polyclonal antibody (∼0.9:1.0 as determined by densitometry; Figure 6B, lanes 2 and 3). As expected, the sample with Myr$^+$ proteins contained less full-length Gag as compared to the sample with Myr$^-$ proteins (∼0.5:1.0) because Myr$^+$ Gag is processed more efficiently (*2*, *11*, *29*). However, when the nitrocellulose membrane used in panel B was analyzed by Western blotting using an anti-CyP A polyclonal antibody (Figure 6C), less CyP A was detected on the beads incubated with the extract prepared from cells expressing the Myr$^+$ Gag protein (lane 2) as compared to the beads incubated with the extract containing the Myr$^-$ Gag (lane 3; CyP A ratio = 0.25:1.0). This amount of CyP A was less than expected whether it was compared to the total CA-related protein detected or to full-length Gag. In contrast, an anti-Tsg101 monoclonal antibody detected amounts of Tsg101 on the beads that were consistent with the amount of Myr$^+$ and Myr$^-$ Gag detected in the immune

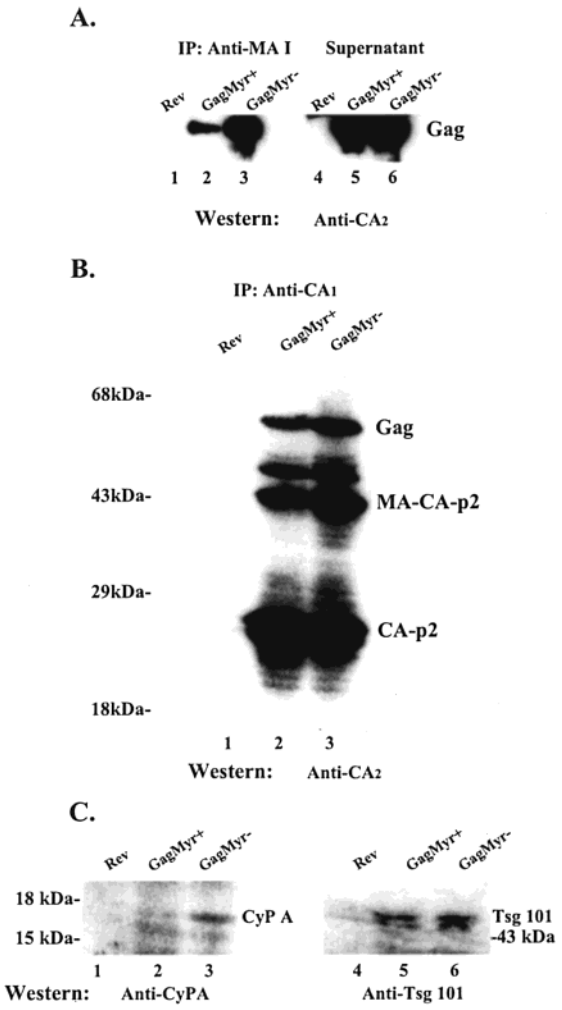

FIGURE 6: Immune-capture of CyP A and Tsg101 by Myr$^+$ and Myr$^-$ Gag. (A) S100 extracts prepared from cells transfected with *rev* alone (lanes 1 and 4), *rev* with wild-type *gag*/*pol* (lanes 2 and 5), or *rev* with Myr$^-$ *gag*/*pol* (lanes 3 and 6) were immunoprecipitated with anti-MA I antibody under the nondenaturating conditions used in Figure 5. The immune-precipitates (lanes 1−3) and aliquots of the supernatants (lanes 4−6) were analyzed by SDS−PAGE followed by Western blotting with anti-CA monoclonal antibody (anti-CA$_2$). (B, C) Protein A agarose beads coated with anti-CA polyclonal antibody and incubated with S100 extracts prepared from cells transfected with *rev* alone (lane 1), *rev* with Myr$^+$ *gag*/*pol* (lane 2), or *rev* with Myr$^-$ *gag*/*pol* (lane 3) were examined by SDS−PAGE, and the same nitrocellulose membrane was analyzed by Western blotting with (B) anti-CA monoclonal antibody (lanes 1−3), (C) polyclonal anti-CyP A antibody (lanes 1−3), or with anti-Tsg101 mouse monoclonal antibody (lanes 4−6).

precipitate (~0.5:1.0; lanes 5 and 6). The results suggest that the presence or absence of the N-terminal myristate moiety influenced the accessibility of the CyP A binding site in the downstream CA domain but not the C-terminal Tsg101 binding region in p6. The myristic acid moiety may have affected the conformation or the multimerization state of regions in Gag beyond the MA domain.

DISCUSSION

In this report, we demonstrated that myristylated wild-type and unmyristylated mutant MA that are prematurely cleaved from $Pr55^{Gag}$ precursors in the cytoplasm form complexes that exhibit different membrane-binding and multimerization properties. Moreover, an antibody directed against an antigenic site near the N-terminal membrane-binding signal differentially recognized the myristylated protein. Structural studies show that recombinant HIV-1 MA has a conserved globular core of clustered helices joined by loops or regions of extended structure. It is reasonable to assume that, following co-translational modification, the myristyl moiety would be inserted into the protein core and alter the disposition of helices (*54*). The lack of antibody recognition that we observed for the myristylated MA protein (Figure 5) could not be only attributed to occlusion by the myristyl group of antigenic sites in the core structure. The CyP A binding site in the downstream CA domain of Gag was also less accessible (Figure 6). Rather, the lack of antibody recognition might reflect differences in the positioning of residues in the MA antigenic site because of the presence of the myristyl group or an influence on the multimerization state of the protein, which obscured the MA and the CA antigenic sites.

The anti-MA I antigenic site (within residues 11−25) is part of 36 structurally equivalent positions in the crystal structures of the HIV-1, simian immunodeficiency virus (SIV), and bovine leukemia virus (BLV) MA protein (*25*). The conserved topology in the 3-dimensional structure is particularly striking since HIV/SIV and BLV exhibit negligible sequence identity. The 36 positions are predicted to form the trimer face, and since myristylation affects multimerization (ref *55* and Figures 2 and 3), may explain why the core region might be structurally distinct in Myr^+ and Myr^- Gag and MA. Indeed, our observations that N-terminal aromatic residues (Figure 4) and the anti-MA I epitope (Figure 5) are exposed differently in the Myr^+ and Myr^- proteins are consistent with previous studies. It is interesting to note that Tyr86, which we found to be inaccessible in both Myr^+ and Myr^- MA (Figure 4) and Cys87 are both involved in the MA membrane targeting function (*56*, *57*) and comprise part of a hydrophobic pocket in the C-terminal region of MA (*21*). Mutations in this pocket alter membrane targeting to the plasma membrane (*57*, *58*). Moreover, prior studies suggest that the entire core is involved in myristate-directed control of membrane-binding and targeting (*2*, *22*, *58*−*62*). Interestingly, the N-terminal region, including the MA I antigenic site, is a key modulator of multimerization of recombinant HIV-1 Gag in vitro (*63*).

Although our results are mainly consistent with previous observations (*20*, *27*, *55*, *62*, *64*), we detected no monomeric MA, and the unmodified MA protein in our cell lysate was in smaller complexes than the myristylated MA protein, in contrast to the results of Morikawa et al. (*55*). Differences in the mode of protein expression and possibly in the cytoplasmic environment provide the most likely explanation for the observed differences. Morikawa et al. expressed the proteins individually as C-terminally His-tagged fusion proteins in bacterial and insect cells and examined their oligomerization state following imidazole elution and purification. We expressed the *gag*, *pol*, and *rev* genes in mammalian cells, permitting proteolytic processing to occur in a more natural setting and assessed protein−protein interactions of MA within cell lysates. Consistent with our observation that Myr^+ Gag formed larger complexes than Myr^- Gag (Figure 3B), the MA protein in the cytosol were detected in larger complexes than unmyristylated MA (Figure 2A). Both homo- and heterotypic interactions are expected to take place in this environment. Interestingly, it has been reported that calmodulin binds peptides containing HIV-1 MA amino acids 11−25 and 31−46 (*65*). Perhaps the inaccessibility of this region of Myr^+ MA to both chymotrypsin digestion and to anti-MA I (Figures 4 and 5) reflects the association of calmodulin or other host proteins with Myr^+ MA in the cytosol.

In our studies, myristate appeared to enhance the membrane binding of MA to a slightly greater extent than it increased the binding of Gag. It is difficult to know if this difference between Gag and MA is significant because the binding of Myr^+ Gag and Myr^+ MA proteins were not assessed with the same probe (i.e., anti-MA was used to tag MA; anti-CA was used to tag Gag). However, the observed differences between the Myr^+ and the Myr^- Gag and MA were also modest (3- vs 2-fold), and these observations were highly reproducible. Indeed, the difference in membrane binding between the Myr^+ and Myr^- proteins may be underestimated since the myristyl switch model predicts that mature Myr^+ MA should exist partially in a state where the myristate is sequestered. The membrane binding affinity of this form of Myr^+ MA is predicted to be less than that of Myr^+ MA with an exposed fatty acid moiety. This makes the observation that the Myr^+ Gag and MA proteins exhibited similar membrane-binding properties (35 and 40 μM, respectively) unexpected and also suggests that the myristic acid moiety is unavailable in our cytosolic Myr^+ Gag as it appears to be in HTLV-1 Gag, which remains soluble and unattached to internal membranes in the cytoplasm (*33*). The myristyl switch hypothesis predicts that Myr^+ Gag should bind better than Myr^+ MA, and in accordance with the model, previous studies from our lab and others demonstrated higher membrane-binding affinity for Gag than for MA (*17*, *27*, *28*, *66*). Since our prior studies and others were done in vitro and/or utilized mostly unmyristylated recombinant proteins, it is likely that protein−protein interactions mediated through regions in MA (*28*, *55*) and the downstream CA and NC domains in the Gag precursor (*6*, *57*, *67*−*69*) account for the differences observed in the more natural setting of the cytoplasm. This notion is supported by the fact that the MA protein was a monomer in our previous studies where recombinant unmyristylated Gag exhibited higher membrane binding affinity than MA (*27*). If, as indicated by our data, the two cytosolic proteins have similar membrane-binding properties in their natural multimerized states, conformational differences in the proteins because of se-

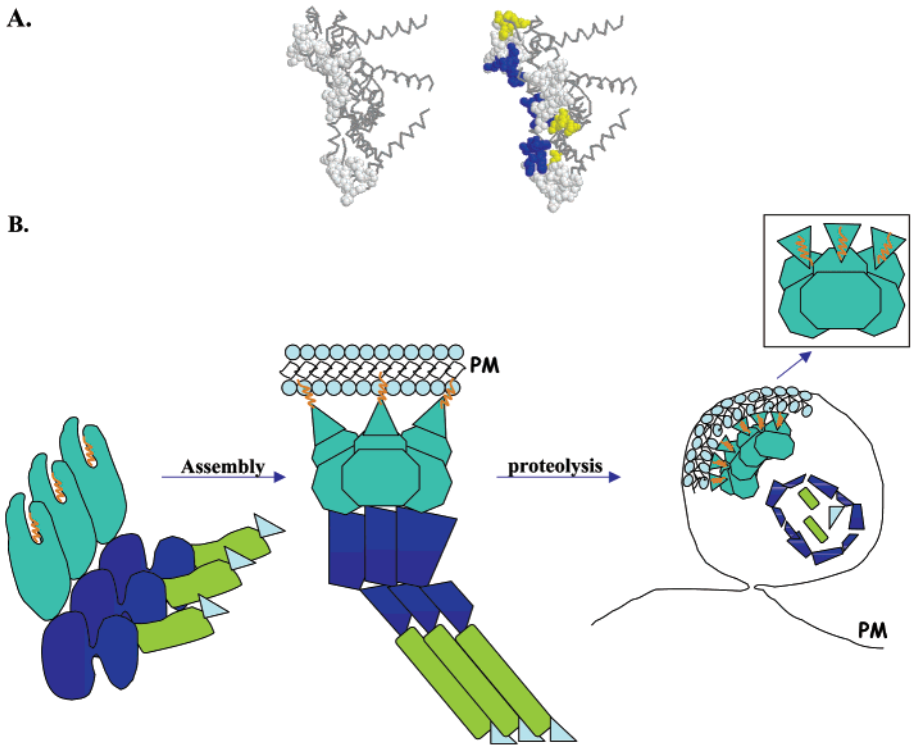

FIGURE 7: Models for structural (A) and functional (B) changes in MA as a result of its co-translation modification by myristylation. The model in panel A suggests specific residues altered in the context of the MA trimer model of Hill et al. (*20*) and is based on the results described in the text. Left: the residues that affect membrane interaction and are predicted to form membrane-binding platform (ref *23* and references therein) are indicated by space-filling. Right: the space-filled residues that comprise the antigen site recognized by anti-MA I are indicate in blue. These residues were differentially exposed in the experiment described in Figure 5. The space-filled residues in yellow show the chymotrypsin substrates protected from proteolysis in the experiment described in Figure 4. The model in panel B illustrates how Gag myristylation and multimerization may drive assembly and maturation.

questration of myristate, multimerization, or both might account for their distinct targeting and functional properties.

Our results, summarized in the model in Figure 7, suggest that regions flanking the N-terminal basic motif are not available in the myristylated proteins as a consequence of the occlusion of the myristate moiety in the cytoplasmic milieu. Occlusion might be due to sequestration within the protein structure or to multimerization of the protein. Consistent with the idea of myristate occlusion (because of folding or multimerization), the HTLV-1 Gag protein was found to be cytosolic even though it is myristylated like the HIV-1 Gag protein (*33*), as noted above. The authors concluded that the modification was unavailable for membrane binding. Amino acids in HIV-1 MA influenced by the modification based on our studies are shown in the context of the current structural model for the unmyristylated recombinant MA protein (Figure 7A). Following transport of Gag to the plasma membrane, the myristate moiety becomes exposed, and the protein undergoes proximal (Figures 4 and 5) and distal (Figure 6) structural changes that facilitate further multimerization (Figures 2, 3, and Figure 7B), consistent with a study showing modulation of particle assembly by phospholipids (*63*). After budding, the mature MA protein, newly generated by proteolytic maturation, adopts a new conformation that sequesters some or all of the myristate in preparation for capsid disassembly. This model is in accordance with the myristyl switch model but suggests that the switch plays a role at a late stage in viral maturation where MA release from the membrane sets the stage for post-assembly events rather than driving membrane-binding during assembly. Thus, myristylation may contribute to conformational properties that increase Gag's membrane affinity not solely through direct contact between myristate and lipids but also by stabilization of tertiary and quartenary protein states that favor formation of larger complexes and viral particle assembly.

ACKNOWLEDGMENT

We thank S. Goff, L. Ehrlich, E. Gottwein, and A. Goff for helpful suggestions and reading of the manuscript. Anti-MA I antibody was a generous gift of R. Schroenbrunner (Roche).

REFERENCES

1. Bryant, M., and Ratner, L. (1990) *Proc. Natl. Acad. Sci. U.S.A. 87*, 523−7.
2. Zhou, W., Parent, L. J., Wills, J. W., and Resh, M. D. (1994) *J. Virol. 68*, 2556−69.
3. Nguyen, D. H., and Hildreth, J. E. (2000) *J. Virol. 74*, 3264−72.
4. Copeland, N. G., Jenkins, N. A., Nexo, B., Schultz, A. M., Rein, A., Mikkelsen, T., and Jorgensen, P. (1988) *J. Virol. 62*, 479−87.
5. Gottlinger, H. G., Sodroski, J. G., and Haseltine, W. A. (1989) *Proc. Natl. Acad. Sci. U.S.A. 86*, 5781−5.
6. Spearman, P., Wang, J. J., Vander Heyden, N., and Ratner, L. (1994) *J. Virol. 68*, 3232−42.
7. Gelderblom, H. R., Ozel, M., and Pauli, G. (1989) *Arch. Virol. 106*, 1−13.
8. Ozel, M., Pauli, G., and Gelderblom, H. R. (1988) *Arch. Virol. 100*, 255−66.

9. Bukrinsky, M. I., Sharova, N., McDonald, T. L., Pushkarskaya, T., Tarpley, W. G., and Stevenson, M. (1993) *Proc. Natl. Acad. Sci. U.S.A. 90*, 6125−9.
10. Gallay, P., Swingler, S., Aiken, C., and Trono, D. (1995) *Cell 80*, 379−88.
11. Fouchier, R. A., Meyer, B. E., Simon, J. H., Fischer, U., and Malim, M. H. (1997) *EMBO J. 16*, 4531−9.
12. Dorfman, T., Mammano, F., Haseltine, W. A., and Gottlinger, H. G. (1994) *J. Virol. 68*, 1689−96.
13. Hermida-Matsumoto, L., and Resh, M. D. (1999) *J. Virol. 73*, 1902−8.
14. Spearman, P., Horton, R., Ratner, L., and Kuli-Zade, I. (1997) *J. Virol. 71*, 6582−92.
15. Yu, X., Yuan, X., Matsuda, Z., Lee, T. H., and Essex, M. (1992) *J. Virol. 66*, 4966−71.
16. Peitzsch, R. M., and McLaughlin, S. (1993) *Biochemistry 32*, 10436−43.
17. Ehrlich, L. S., Fong, S., Scarlata, S., Zybarth, G., and Carter, C. (1996) *Biochemistry 35*, 3933−43.
18. Parent, L. J., Wilson, C. B., Resh, M. D., and Wills, J. W. (1996) *J. Virol. 70*, 1016−26.
19. Le Blanc, I., Rosenberg, A. R., and Dokhelar, M. C. (1999) *J. Virol. 73*, 1860−7.
20. Hill, C. P., Worthylake, D., Bancroft, D. P., Christensen, A. M., and Sundquist, W. I. (1996) *Proc. Natl. Acad. Sci. U.S.A. 93*, 3099−104.
21. Massiah, M. A., Worthylake, D., Christensen, A. M., Sundquist, W. I., Hill, C. P., and Summers, M. F. (1996) *Protein Sci. 5*, 2391−8.
22. Matthews, S., Barlow, P., Clark, N., Kingsman, S., Kingsman, A., and Campbell, I. (1995) *Biochem. Soc. Trans. 23*, 725−9.
23. Christensen, A. M., Massiah, M. A., Turner, B. G., Sundquist, W. I., and Summers, M. F. (1996) *J. Mol. Biol. 264*, 1117−31.
24. Conte, M. R., Klikova, M., Hunter, E., Ruml, T., and Matthews, S. (1997) *EMBO J. 16*, 5819−26.
25. Matthews, S., Mikhailov, M., Burny, A., and Roy, P. (1996) *EMBO J. 15*, 3267−74.
26. Rao, Z., Belyaev, A. S., Fry, E., Roy, P., Jones, I. M., and Stuart, D. I. (1995) *Nature 378*, 743−7.
27. Scarlata, S., Ehrlich, L. S., and Carter, C. A. (1998) *J. Mol. Biol. 277*, 161−9.
28. Morikawa, Y., Hockley, D. J., Nermut, M. V., and Jones, I. M. (2000) *J. Virol. 74*, 16−23.
29. Hatanaka, H., Iourin, O., Rao, Z., Fry, E., Kingsman, A., and Stuart, D. I. (2002) *J. Virol. 76*, 1876−83.
30. Provitera, P., Bouamr, F., Murray, D., Carter, C., and Scarlata, S. (2000) *J. Mol. Biol. 296*, 887−98.
31. Wilcox, C., Hu, J. S., and Olson, E. N. (1987) *Science 238*, 1275−8.
32. Buss, J. E., Kamps, M. P., and Sefton, B. M. (1984) *Mol. Cell. Biol. 4*, 2697−704.
33. Le Blanc, I., Blot, V., Bouchaert, I., Salamero, J., Goud, B., Rosenberg, A. R., and Dokhelar, M. C. (2002) *J. Virol. 76*, 905−11.
34. Tanaka, T., Ames, J. B., Harvey, T. S., Stryer, L., and Ikura, M. (1995) *Nature 376*, 444−7.
35. Ames, J. B., Ishima, R., Tanaka, T., Gordon, J. I., Stryer, L., and Ikura, M. (1997) *Nature 389*, 198−202.
36. Ames, J. B., Tanaka, T., Stryer, L., and Ikura, M. (1994) *Biochemistry 33*, 10743−53.
37. Geyer, M., Munte, C. E., Schorr, J., Kellner, R., and Kalbitzer, H. R. (1999) *J. Mol. Biol. 289*, 123−38.
38. Chow, M., Newman, J. F., Filman, D., Hogle, J. M., Rowlands, D. J., and Brown, F. (1987) *Nature 327*, 482−6.
39. Moscufo, N., and Chow, M. (1992) *J. Virol. 66*, 6849−57.
40. Fackler, O. T., Kienzle, N., Kremmer, E., Boese, A., Schramm, B., Klimkait, T., Kucherer, C., and Mueller-Lantzsch, N. (1997) *Eur. J. Biochem. 247*, 843−51.
41. Smith, A. J., Cho, M. I., Hammarskjold, M. L., and Rekosh, D. (1990) *J. Virol. 64*, 2743−50.
42. Ebbets-Reed, D. (1996) Ph.D. Thesis, p 209, State University of New York at Stony Brook, Stony Brook, NY.
43. Mergener, K., Facke, M., Welker, R., Brinkmann, V., Gelderblom, H. R., and Krausslich, H. G. (1992) *Virology 186*, 25−39.
44. Alland, L., Peseckis, S. M., Atherton, R. E., Berthiaume, L., and Resh, M. D. (1994) *J. Biol. Chem. 269*, 16701−5.
45. Ehrlich, L. S., Krausslich, H. G., Wimmer, E., and Carter, C. A. (1990) *AIDS Res. Hum. Retroviruses 6*, 1169−75.
46. Hope, M. J., Bally, M. B., Webb, G., and Cullis, P. R. (1985) *Biochim. Biophysic. Acta 812*, 55−65.
47. Tritel, M., and Resh, M. D. (2001) *J. Virol. 75*, 5473−81.
48. Ebbets-Reed, D., Scarlata, S., and Carter, C. A. (1996) *Biochemistry 35*, 14268−75.
49. Hirayama, K., Akashi, S., Furuya, M., and Fukuhara, K. (1990) *Biochem. Biophys. Res. Commun. 173*, 639−46.
50. Titani, K., Koide, A., Hermann, J., Ericsson, L. H., Kumar, S., Wade, R. D., Walsh, K. A., Neurath, H., and Fischer, E. H. (1977) *Proc. Natl. Acad. Sci. U.S.A. 74*, 4762−6.
51. Yao, J., Dey, M., Pastor, S. J., and Wilkins, C. L. (1995) *Anal. Chem. 67*, 3638−42.
52. Luban, J., Bossolt, K. L., Franke, E. K., Kalpana, G. V., and Goff, S. P. (1993) *Cell 73*, 1067−78.
53. Ver Plank, L., Bouamr, F., LaGrassa, T., Agresta, B., Kikonyogo, A., Leis, J., Carter, C. A. (2001) *Proc. Natl. Acad. Sci. U.S.A., 48*, 7724−7729.
54. Liemann, S., Chandran, K., Baker, T. S., Nibert, M. L., and Harrison, S. C. (2002) *Cell 108*, 283−95.
55. Morikawa, Y., Zhang, W. H., Hockley, D. J., Nermut, M. V., and Jones, I. M. (1998) *J. Virol. 72*, 7659−63.
56. Ono, A., Huang, M., and Freed, E. O. (1997) *J. Virol. 71*, 4409−18.
57. Ono, A., Orenstein, J. M., and Freed, E. O. (2000) *J. Virol. 74*, 2855−66.
58. Freed, E. O., Orenstein, J. M., Buckler-White, A. J., and Martin, M. A. (1994) *J. Virol. 68*, 5311−20.
59. Ono, A., and Freed, E. O. (1999) *J. Virol. 73*, 4136−44.
60. Paillart, J. C., and Gottlinger, H. G. (1999) *J. Virol. 73*, 2604−12.
61. Zhou, W., and Resh, M. D. (1996) *J. Virol. 70*, 8540−8.
62. Nermut, M. V., Hockley, D. J., Bron, P., Thomas, D., Zhang, W. H., and Jones, I. M. (1998) *J. Struct. Biol. 123*, 143−9.
63. Campbell, S., Fisher, R. J., Towler, E. M., Fox, S., Issaq, H. J., Wolfe, T., Phillips, L. R., and Rein, A. (2001) *Proc. Natl. Acad. Sci. U.S.A. 98*, 10875−9.
64. Nermut, M. V., Hockley, D. J., Jowett, J. B., Jones, I. M., Garreau, M., and Thomas, D. (1994) *Virology 198*, 288−96.
65. Radding, W., Williams, J. P., McKenna, M. A., Tummala, R., Hunter, E., Tytler, E. M., and McDonald, J. M. (2000) *AIDS Res. Hum. Retroviruses 16*, 1519−25.
66. Spearman, P., Horton, R., Ratner, L., and Kuli-Zade, I. (1997) *J. Virol. 71*, 6582−92.
67. Sandefur, S., Smith, R. M., Varthakavi, V., and Spearman, P. (2000) *J. Virol. 74*, 7238−49.
68. Sandefur, S., Varthakavi, V., and Spearman, P. (1998) *J. Virol. 72*, 2723−32.
69. Wang, J. J., Sandefur, S., Spearman, P., Chiou, C. T., Chiang, P. H., and Ratner, L. (2001) *Appl. Immunohistochem. Mol. Morphol. 9*, 371−9.

BI020692Z